Biochemical and Biophysical Research Communications 524 (2020) 340–345

Contents lists available at ScienceDirect

Biochemical and Biophysical Research Communications

journal homepage: www.elsevier.com/locate/ybbrc

Dual real-time *in vivo* monitoring system of the brain-gut axis

Yuya Nishimura [a], Yota Fukuda [b, c], Toya Okonogi [a], Soichiro Yoshikawa [d, e], Hajime Karasuyama [d], Naomi Osakabe [b], Yuji Ikegaya [a, f], Takuya Sasaki [a, g], Takahiro Adachi [c, *]

[a] Graduate School of Pharmaceutical Sciences, The University of Tokyo, 7-3-1 Hongo Bunkyo-ku, Tokyo, 113-0033, Japan
[b] Department of Bio-science and Engineering, Shibaura Institute of Technology, Saitama, Saitama, 337-5780, Japan
[c] Department of Immunology, Medical Research Institute, Tokyo Medical and Dental University, Tokyo, 113-8510, Japan
[d] Department of Immune Regulation, Graduate School, Tokyo Medical and Dental University, Tokyo, 113-8519, Japan
[e] Department of Cellular Physiology, Okayama University Graduate School of Medicine, Dentistry, and Pharmaceutical Sciences, Okayama, 700-8558, Japan
[f] Center for Information and Neural Networks, Suita, Osaka, 565-0871, Japan
[g] Precursory Research for Embryonic Science and Technology (PRESTO), Japan Science and Technology Agency (JST), Kawaguchi, Saitama, 332-0012, Japan

ARTICLE INFO

Article history:
Received 10 January 2020
Accepted 14 January 2020
Available online 26 January 2020

Keywords:
Ca^{2+} signaling
Brain-gut axis
Electrophysiology
Imaging
Capsaicin

ABSTRACT

The brain–gut axis which is an interaction between recognition and emotion and the gut sensory system for food and microbiota is important for health. However, there is no real-time monitoring system of the brain and the gut simultaneously so far. We attempted to establish a dual real-time monitoring system for the brain–gut axis by a combination of intravital Ca^{2+} imaging of the gut and electroencephalogram. Using a conditional Yellow Cameleon 3.60 expression mouse line, we performed intravital imaging of the gut, electrophysiological recordings of the vagus nerve, and electroencephalogram recordings of the various cortical regions simultaneously upon capsaicin stimuli as a positive control. Upon capsaicin administration into the small intestinal lumen, a simultaneous response of Ca^{2+} signal in the enteric nervous system and cortical local field potentials (LFPs) was successfully observed. Both of them responded immediately upon capsaicin stimuli. Capsaicin triggered a significant increase in the frequency of vagus nerve spikes and a significant decrease in the slow-wave power of cortical LFPs. Furthermore, capsaicin induced delayed and sustained Ca^{2+} signal in intestinal epithelial cells and then suppressed intestinal motility. The dual real-time monitoring system of the brain and the gut enables to dissect the interaction between the brain and the gut over time with precision.

1. Introduction

Gut sensory functions are important for the control of gut motility, hormone and antimicrobial peptide secretion, and so on [1–5]. In addition to the gut itself, the brain also senses nutrients in food and fluid in the gut via sensory neurons [6,7]. The gut environmental conditions are tightly linked to health and disease [8–10]. Indeed, a dysfunction of these has been shown to evoke neural disorders such as irritable bowel syndrome [11], autism spectrum disorders [8,12], and Parkinson's disease [13]. Thus, bidirectional interactions between the brain and the gut are crucial for health maintenance.

To elucidate the brain–gut axis in health and disease, brain activity *in vivo* can be monitored by electroencephalogram, Ca^{2+} imaging, and functional magnetic resonance imaging. We have also established a recording method that comprehensively monitors collective neuronal activity of multiple brain regions using a multichannel recording device for the simultaneous monitoring of local field potential (LFP) signals from brain regions [14,15]. Brain LFP signals represent the collective activity of neuronal and synaptic populations, which are used as a measure to estimate psychiatric and arousal states of experimental animals. In contrast to the brain, so far, the *in vivo* analysis of the gut is rare due to limited methodology. Therefore, the gut-sensing mechanisms for foods and microbiota remain unclear. Recently, we have established an intravital imaging system of Ca^{2+} dynamics in intestinal epithelial cells (IECs) by using the Ca^{2+} biosensor Yellow Cameleon 3.60

* Corresponding author. Department of Immunology, Medical Research Institute, Tokyo Medical and Dental University, 1-5-45 Yushima, Bunkyo-ku, Tokyo, 113-8510, Japan.
E-mail address: tadachi.imm@mri.tmd.ac.jp (T. Adachi).

https://doi.org/10.1016/j.bbrc.2020.01.090
0006-291X/

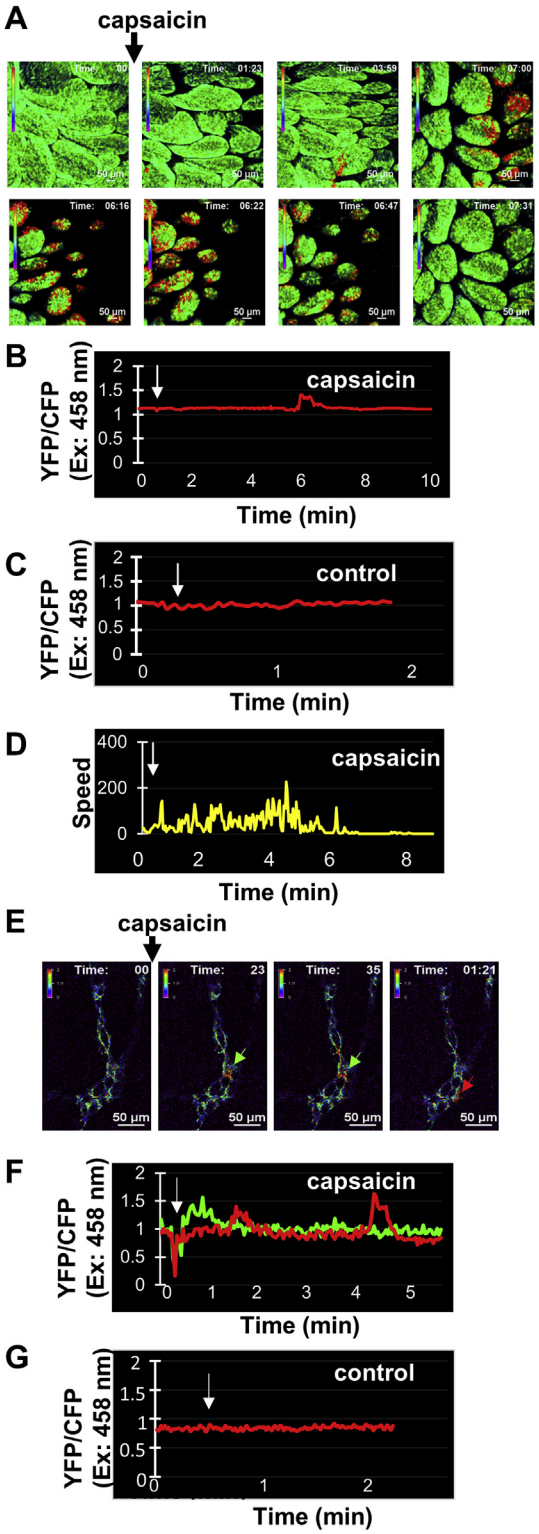

Fig. 1. Intravital Ca^{2+} signal images mediated by capsaicin in the intestinal tract. (A) Representative Ca^{2+} signal images in the intestinal tract of an ubiquitous YC3.60 expression mouse. Ratiometric images (YFP/CFP excitation at 458 nm) are shown. Capsaicin in PBS (1 mM) was added at the indicated time point. A rainbow parameter indicates relative Ca^{2+} concentrations. Scale bar, 50 μm; frame = 216. (B) Time course for the fluorescence intensities of the YFP/CFP ratio on excitation at 458 nm in the intestinal epithelium in (A) and its control added PBS only (C). (D) Time course for of the speed of the intestinal epithelium in (A). (E) Representative Ca^{2+} signal images in the intestinal tract of a Nestin-Cre/YC3.60 mouse. Ratiometric images (YFP/CFP excitation at 458 nm) before and after the addition of capsaicin are shown. A rainbow parameter indicates relative Ca^{2+} concentrations. Scale bar, 50 μm; frame = 143. (F) Time course for the fluorescence intensities of the YFP/CFP ratio on excitation at 458 nm in the myenteric plexus marked in (E) and its control added PBS only (G). Capsaicin in PBS (1 mM) or PBS only was added at the indicated time point.

(YC3.60) expression mouse line [16,17]. We also established a visualization system of Ca^{2+} dynamics in enteric nervous system (ENS) cells *in vivo*. However, there is no real-time monitoring system of the gut and the brain simultaneously so far. Therefore, we tried to establish a system to assess the activities of both the brain and the gut in real-time. In the combination of electroencephalogram and intravital Ca^{2+} imaging in the gut, we show here how to monitor the gut-mediated sensory responses of the brain and the gut *in vivo* simultaneously.

2. Materials and methods

2.1. Mice

The nerve cell-specific YC3.60 expression line ($YC3.60^{flox}$/Nestin-Cre) and the ubiquitous YC3.60 expression line ($YC3.60^{flox}$/CAG-Cre) have been previously described [17]. These mice were maintained in our animal facility under specific pathogen-free conditions in accordance with the guidelines of the Tokyo Medical and Dental University for Animal Care. For electrophysiological recordings, male C57BL/6 mice (6–10 weeks old) were used in this study. These procedures have been approved by the Committee of the Tokyo Medical and Dental University for Animal Care (approval number A2019-207A) and the Experimental Animal Ethics Committee at the University of Tokyo (approval number P24-70).

2.2. Cells

Ubiquitous YC3.60 expression mice [17] were euthanized by cervical dislocation and their dorsal root ganglia (DRG) cells and nodose ganglia (NG) were excised. The DRG or NG were treated with 1 mg/mL collagenase and 0.25 mg/mL trypsin as described previously [18]. After pipetting, the cells were washed with the medium twice and cultured at 37 °C on a gelatin-coated plate with Dulbecco's modified Eagle's medium containing 10% fetal calf serum and 100 ng/mL nerve growth factor.

2.3. Intravital imaging

IECs from anesthetized mice were imaged. Small intestinal tracts were exposed, surgically opened lengthwise, placed on a cover glass and immobilized on a microscope stage as described previously [16]. Alternatively, small intestinal tracts were exposed, placed on a cover glass and immobilized on a microscope stage. For image acquisition, a Nikon A1 laser scanning confocal microscope with a 20 × objective and NIS-Elements AR software was used as described previously [16]. Images of purified neurons in PBS were also obtained as described above. The acquired images were analyzed with NisElements software (Nikon), and obtained time course of intracellular Ca^{2+} concentration and the cell movement speed.

2.4. Electrophysiological recording

Mice were anesthetized with urethane (1.0 g/kg, intraperitoneal injection) and restrained with their head held in place by a metal plate. For vagus nerve recording, an incision was made in the left neck area from the larynx to the sternum, and the left cervical vagus nerve was isolated. The isolated nerve was enclosed by a cuff-shaped electrode (Unique Medical Co., Ltd., Japan; inner

diameter = 0.5–1.0 mm, electrode area = 0.25 mm^2, cathode-anode interval = 1.5–2.0 mm, and total length 4.0 mm). For brain recording, a craniotomy was performed to create a hole (2.0 × 2.0 mm^2) centered at 1.4 mm posterior and 1.4 mm lateral to the bregma using a high-speed drill, and the dura was surgically removed. Two stainless steel screws were implanted in the bone above the cerebellum to serve as ground and reference electrodes. Signal electrode wires were constructed from a 17-μm-wide polyimide-coated platinum-iridium (90%–10%) wire (California Fine Wire), and the electrode tips were plated with platinum to lower the electrode impedances to 150–300 kΩ at 1 kHz. An electrode assembly consisting of six signal electrode wires, designed and created using a three-dimensional printer (UP Plus 2; Delta Micro Factory Corporation), was inserted into the exposed area at a speed of 10 μm/s. The length of the individual electrodes was adjusted so that the final depth in the brain ranged from 500 to 2000 μm. The electrodes were allowed to stabilize at their final position for 30 min before recording began. Small intestinal tracts were then exposed and surgically opened directly for drug injection. Each mouse was connected to the recording equipment via Cereplex M (Blackrock), a digitally programmable amplifier. The headstage output was conducted via a lightweight multiwire tether to the Cereplex Direct recording system (Blackrock), a data acquisition system. LFP recordings were sampled at 2 kHz and filtered between 0 and 2 and 500 Hz.

2.5. Data analysis

For the vagus nerve signals, a spike unit was detected when the amplitude of a negative deflection of the extracellularly recorded signals exceeded a threshold of 5 standard deviations from the baseline during quiescent periods. For the brain signals, the power spectra of LFP signals were convolved by a Morlet's wavelet family or calculated by fast Fourier transformation using Matlab. The power of LFPs in the following sub-frequency bands was calculated: slow-wave (0.2–1 Hz), delta (1–2 Hz), theta (4–10 Hz), slow-gamma (25–60 Hz), and fast-gamma (80–140 Hz). The baseline power for statistical comparisons was defined as LFP power 0–2 min before the application of the drug. All values are reported as the mean ± SEM.

3. Results

3.1. Capsaicin elicited in vitro Ca^{2+} signals in DRG-derived and NG-derived neurons from CAG-Cre/YC3.60^{flox} mice

Capsaicin is a well-known ingredient in hot peppers and stimulates transient receptor potential vanilloid subfamily member 1 (TRPV1), which is expressed in some neurons, including sensory neurons [19] and IECs [20]. Capsaicin induces Ca^{2+} flux via TRPV1 in sensory neurons [21] and activates brown adipocytes [22]. At first, we tested whether the Ca^{2+} biosensor YC3.60 is suitable for the detection of capsaicin-mediated Ca^{2+} dynamics in the sensory neurons. We prepared neurons from the DRG of ubiquitous YC3.60 expression mice [17], cultured the neurons on a dish for several days, and then examined their Ca^{2+} responses to capsaicin. Capsaicin induced robust Ca^{2+} signals in primary neural cells derived from DRG (Supplementary Figs. 1A–C). Furthermore, we examined neurons from NG because subpopulations of NG express TRPV1 which recognizes capsaicin [23]. Capsaicin induced robust Ca^{2+} signals in primary neural cells derived from NG (Supplementary Figs. 1D–F). Thus, the YC3.60 expression mouse line is adequate for the evaluation of capsaicin-mediated signals in sensory neurons.

3.2. Capsaicin elicited Ca^{2+} signals in enteric epithelial cells and myenteric plexus in vivo

Next, we tested whether capsaicin induces Ca^{2+} signals in IECs, as TRPV1 is expressed in IECs [20]. Intravital imaging of the intestine in ubiquitous YC3.60 expression mice revealed transient Ca^{2+} signals after the application of capsaicin (Fig. 1A; Supplementary video 1). Capsaicin induced a relatively long period of Ca^{2+} signals in IECs, although it was induced retardely after stimulation (Fig. 1B and C). Furthermore, capsaicin inhibited the local movement of the intestinal tract after Ca^{2+} signals in IECs (Fig. 1D). We also investigated capsaicin-mediated Ca^{2+} signals in the myenteric plexus. Capsaicin induced Ca^{2+} signals in the myenteric plexus immediately upon stimulation (Fig. 1E and F; Supplementary video 2). Furthermore, capsaicin also induced delayed Ca^{2+} signals in other cells. These results indicate that capsaicin induced a biphasic Ca^{2+} signals in the myenteric plexus.

3.3. Capsaicin transiently increases vagus nerve spike bursts

To examine whether the observed capsaicin-induced Ca^{2+} responses were transmitted to the nervous system, we directly

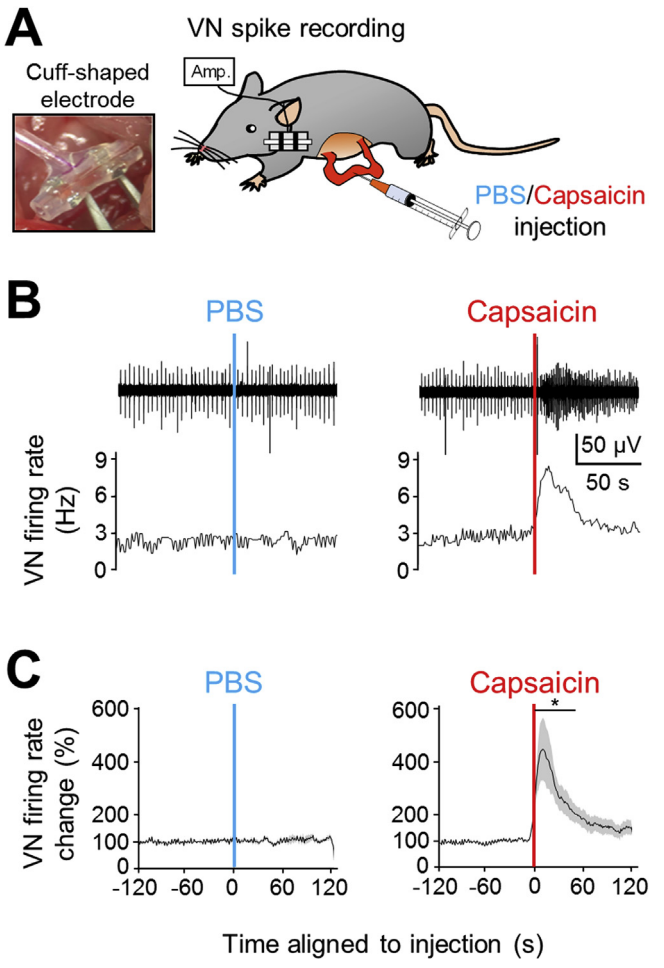

Fig. 2. Capsaicin-induced changes in vagus nerve spikes. (A) Schematic illustration. (B) (Top) Representative vagus nerve action potential traces high-pass filtered at 300 Hz aligned to the timing of injection of PBS (left) or capsaicin (right) into the jejunum. (Bottom) Instantaneous vagus nerve firing rates corresponding to the top traces. (C) Averaged time changes in the vagus nerve firing rates (n = 5 mice). Data were normalized to the firing rates at 0–2 min before the drug injection. The asterisk represents a significant increase ($p < 0.05$, paired t-test) in vagus nerve firing rates at 0–60 s after the injection.

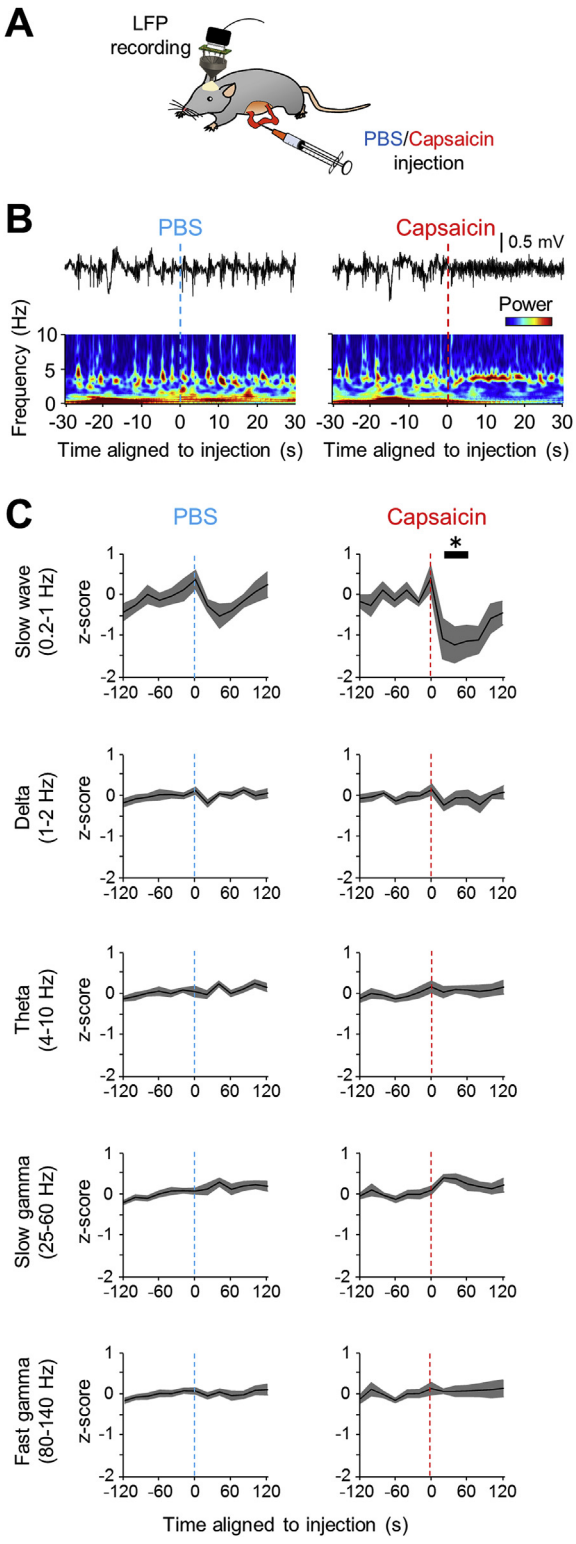

Fig. 3. Capsaicin-induced changes in cortical LFP power. (A) Schematic illustration. (B) (top) Representative hippocampal LFP traces bandpass filtered at 1–150 Hz aligned to the timing of injection of PBS (left) or capsaicin (right) into the jejunum. (Bottom) Power spectra constructed from LFP traces. Note the injection-triggered changes in LFP power at <1 Hz after capsaicin injection. (C) Averaged time changes in z-scored LFP power at individual frequency bands ($n = 7$ mice). Data were normalized to the power at 0–2 min before drug injection. The asterisk represents a significant reduction in LFP power at 20–60 s after injection.

recorded electrical spiking activity from the left cervical vagus nerve using a cuff-shaped electrode, while capsaicin was injected into the gut (Fig. 2A and B). The frequency of vagus nerve spikes was significantly increased up to 60 s after capsaicin injection ($t_4 = 3.90$, $P = 0.018$, paired t-test compared to that 0–2 min before the injection) but not PBS injection ($t_4 = 0.29$, $P = 0.79$) (Fig. 2C). This result confirms that signals generated by capsaicin injection in the jejunum can be transmitted to the cervical vagus nerve.

3.4. Capsaicin reduces cortical LFP power at a slow-wave band

We then recorded neuronal ensemble activity patterns in the mouse brain using *in vivo* extracellular electrophysiological recordings from the neocortex, while capsaicin was injected into the gut (Fig. 3A). Cortical regions generate diverse rhythmic activity, which has been thought to link the firing of single neurons into collective neuronal ensembles [24]. Power spectrum analysis demonstrated that capsaicin injection triggered pronounced changes in LFP power, especially at low-frequency bands of less than 1 Hz (Fig. 3B). To further quantify these changes, we computed cortical LFP power at slow-wave (0.2–1 Hz), delta (1–2 Hz), theta (4–10 Hz), slow-gamma (25–60 Hz), and fast-gamma (80–140 Hz) bands (Fig. 3C). In each recording data, LFP power at each frequency band was converted to z-scores relative to the baseline (0–2 min before drug injection). From the population data, we found a significant reduction in the LFP power specifically at the slow-wave band at 20–60 s after capsaicin injection ($t_6 = 2.95$, $P = 0.026$, paired t-test compared to a z-score of 0) but not PBS injection ($t_6 = 2.09$, $P = 0.081$). Here, the time period of 0–20 s after injection onset was removed from our analysis as the duration of the injection spanned for 5–10 s, which somewhat differed across experiments. The other frequency bands did not show such significant results ($P > 0.05$).

3.5. Capsaicin-induced physiologic responses in the brain and the gut

To precisely dissect the physiological interaction of the brain and the gut, we tried to establish a recording system that allowed us to simultaneously monitor gut Ca^{2+} signals and cortical LFP signals. We performed dual real-time monitoring of gut Ca^{2+} signals and cortical LFP signals in response to capsaicin *in vivo* as shown in Fig. 4A. Capsaicin-induced Ca^{2+} signals in the myenteric plexus and cortical LFP signals were detected almost simultaneously several seconds after the injection of capsaicin into the gut lumen (Fig. 4B). A comparison of the time course between the gut and the brain showed that capsaicin-induced physiological responses co-occurred. Thus, we successfully established a dual real-time monitoring system of the gut and the brain *in vivo*.

4. Discussion

In this study, we established a dual real-time monitoring system of the brain and the gut by a combination of Ca^{2+} signals detection in the gut and extracellular electrophysiological recordings of the brain. Capsaicin induced Ca^{2+} signals in epithelial cells and ENS cells with distinct time courses after stimulation. Furthermore, capsaicin induced delayed and sustained Ca^{2+} signals in IECs followed by the suppression of the local movement of the intestinal epithelium. In addition, we demonstrated that capsaicin reduced cortical LFP power at a slow-wave band in the brain.

Gut-sensing information is transmitted to the central nervous system (CNS) through sensory neurons [2,6,7]. At the same time, the ENS which senses the stimuli in the gut may regulate intestinal motility as the myenteric plexus controls peristalsis in the gut [25].

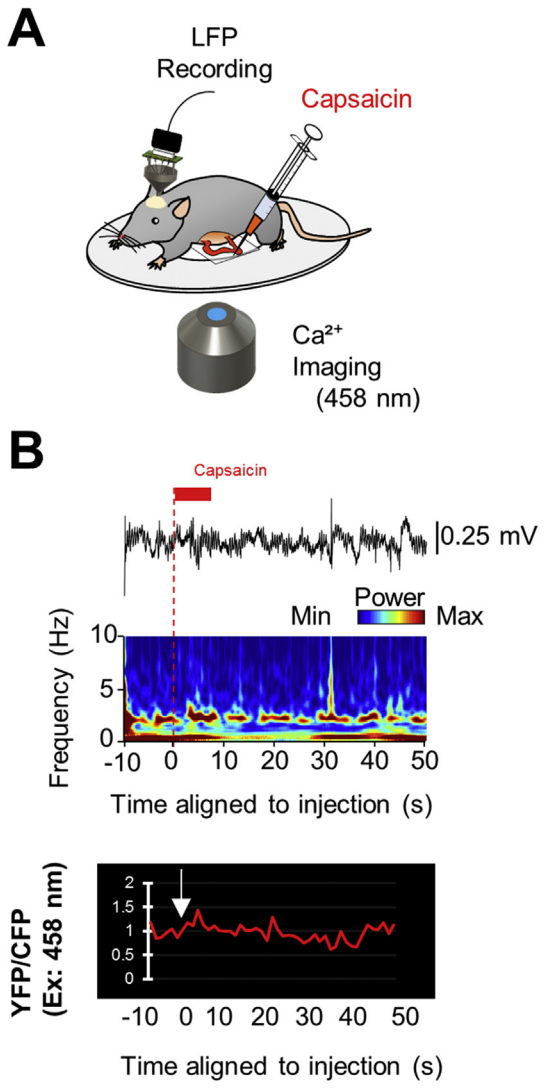

Fig. 4. Simultaneous intravital Ca^{2+} signal imaging of the gut and electrophysiological recording of the brain in response to capsaicin in the YC3.60^{flox}/Nestin-Cre mouse. (A) Schematic illustration. (B) Representative recording data showing the simultaneous monitoring of capsaicin-induced cortical LFP power changes and gut Ca^{2+} signals. (Top) Representative hippocampal LFP trace bandpass filtered at 1–150 Hz aligned to the timing of injection of capsaicin into the jejunum. (Middle) Power spectra constructed from LFP traces. (Bottom) Time course for the fluorescence intensities of the YFP/CFP ratio on excitation at 458 nm in the myenteric plexus. Frame = 47. Capsaicin in PBS (1 mM) was added at the indicated time point.

To fill between the CNS and the ENS, we established a dual real-time monitoring system of the brain–gut axis in this study. The brain–gut axis is important for mental and physiological health [8–11,26], although their details are unknown so far. Our dual real-time monitoring system allows dissecting the relations between the brain and the gut precisely.

We used capsaicin as a positive control to induce signals in the gut and the brain, as the capsaicin receptor TRPV1 is expressed on the neurons and gut epithelial tissues, and various physiological functions have been reported so far [19,27,28]. Indeed, capsaicin evoked Ca^{2+} signals in IECs and ENS cells, although their kinetics are distinct. After Ca^{2+} signals in IECs, capsaicin suppressed the local movement of the intestinal epithelium probably due to the hyperpolarization of the smooth muscle [29]. Furthermore, the kinetics of Ca^{2+} signals mediated by capsaicin in IECs is also distinct from that mediated by probiotics [16]. Thus, the kinetics of Ca^{2+} signals seems to be dependent on the stimuli and may provide a clue to understand its signaling pathway and/or function.

We demonstrated that the injection of capsaicin into the gut lumen induced a transient decrease in the slow-wave power of cortical LFPs in some anesthetized mice. Based on the general assumption that the slow wave of brain signals increases with decreased animal's arousal levels, our data suggest that capsaicin triggered a transient shift of the animal's brain states to higher arousal levels. These data show direct physiological evidence that compounds in the jejunum have the potential to trigger prominent changes in brain activity states, the so-called gut-brain transmission.

Collectively, we established a dual real-time monitoring system of the brain–gut axis *in vivo*. This will be a powerful method to dissect the effect of various food in the intestinal tract on the brain–gut axis with precision and contribute to clarify the interaction between the gut and the brain.

Declaration of competing interest

The authors declare that there is no conflict of interest.

Acknowledgements

We are grateful to Dr. G. Schütz (DKFZ) for the Nestin-Cre mice, Dr. M. Okabe (Osaka University) for the CAG-Cre mice, Dr. A. Miyawaki (RIKEN) for the YC3.60 gene. This work was supported in part by grants from the Ministry of Education, Culture, Sports, Science and Technology of Japan (15K08526 to TA), the Joint Usage/Research Program of Medical Research Institute (TMDU) (to TA, YS, HK, NO), the Naoki Tsuchida Memorial Research Grant (TMDU) (to TA, SY) and the Yamada Research Grant (to TA, TS).

Appendix A. Supplementary data

Supplementary data to this article can be found online at https://doi.org/10.1016/j.bbrc.2020.01.090.

References

[1] C. Alcaino, K.R. Knutson, A.J. Treichel, G. Yildiz, P.R. Strege, D.R. Linden, J.H. Li, A.B. Leiter, J.H. Szurszewski, G. Farrugia, A. Beyder, A population of gut epithelial enterochromaffin cells is mechanosensitive and requires Piezo 2 to convert force into serotonin release, Proc. Natl. Acad. Sci. U. S. A. 115 (2018) E7632–E7641.
[2] D.V. Bohorquez, R.A. Shahid, A. Erdmann, A.M. Kreger, Y. Wang, N. Calakos, F. Wang, R.A. Liddle, Neuroepithelial circuit formed by innervation of sensory enteroendocrine cells, J. Clin. Investig. 125 (2015) 782–786.
[3] G. Burnstock, Purinergic signalling in the gut, Adv. Exp. Med. Biol. 891 (2016) 91–112.
[4] I. Depoortere, Taste receptors of the gut: emerging roles in health and disease, Gut 63 (2014) 179–190.
[5] M.M. Kaelberer, K.L. Buchanan, M.E. Klein, B.B. Barth, M.M. Montoya, X. Shen, D.V. Bohorquez, A gut-brain neural circuit for nutrient sensory transduction, Science 361 (2018).
[6] R.B. Chang, D.E. Strochlic, E.K. Williams, B.D. Umans, S.D. Liberles, Vagal sensory neuron subtypes that differentially control breathing, Cell 161 (2015) 622–633.
[7] E.K. Williams, R.B. Chang, D.E. Strochlic, B.D. Umans, B.B. Lowell, S.D. Liberles, Sensory neurons that detect stretch and nutrients in the digestive system, Cell 166 (2016) 209–221.
[8] T.G. Dinan, J.F. Cryan, The impact of gut microbiota on brain and behaviour: implications for psychiatry, Curr. Opin. Clin. Nutr. Metab. Care 18 (2015) 552–558.
[9] E.A. Mayer, Gut feelings: the emerging biology of gut-brain communication, Nat. Rev. Neurosci. 12 (2011) 453–466.
[10] S.H. Rhee, C. Pothoulakis, E.A. Mayer, Principles and clinical implications of the brain-gut-enteric microbiota axis, Nat. Rev. Gastroenterol. Hepatol. 6 (2009) 306–314.
[11] H. Raskov, J. Burcharth, H.C. Pommergaard, J. Rosenberg, Irritable bowel syndrome, the microbiota and the gut-brain axis, Gut Microb. 7 (2016) 365–383.

[12] A. Azhari, F. Azizan, G. Esposito, A systematic review of gut-immune-brain mechanisms in Autism Spectrum Disorder, Dev. Psychobiol. 61 (5) (2018) 752–771, https://doi.org/10.1002/dev.21803.
[13] T.R. Sampson, J.W. Debelius, T. Thron, S. Janssen, G.G. Shastri, Z.E. Ilhan, C. Challis, C.E. Schretter, S. Rocha, V. Gradinaru, M.F. Chesselet, A. Keshavarzian, K.M. Shannon, R. Krajmalnik-Brown, P. Wittung-Stafshede, R. Knight, S.K. Mazmanian, Gut microbiota regulate motor deficits and neuroinflammation in a model of Parkinson's disease, Cell 167 (2016) 1469–1480 e1412.
[14] D. Konno, R. Nakayama, M. Tsunoda, T. Funatsu, Y. Ikegaya, T. Sasaki, Collection of biochemical samples with brain-wide electrophysiological recordings from a freely moving rodent, J. Pharmacol. Sci. 139 (2019) 346–351.
[15] T. Sasaki, Y. Nishimura, Y. Ikegaya, Simultaneous recordings of central and peripheral bioelectrical signals in a freely moving rodent, Biol. Pharm. Bull. 40 (2017) 711–715.
[16] T. Adachi, S. Kakuta, Y. Aihara, T. Kamiya, Y. Watanabe, N. Osakabe, N. Hazato, A. Miyawaki, S. Yoshikawa, T. Usami, H. Karasuyama, H. Kimoto-Nira, K. Hirayama, N.M. Tsuji, Visualization of probiotic-mediated Ca(2+) signaling in intestinal epithelial cells in vivo, Front. Immunol. 7 (2016) 601.
[17] S. Yoshikawa, T. Usami, J. Kikuta, M. Ishii, T. Sasano, K. Sugiyama, T. Furukawa, E. Nakasho, H. Takayanagi, T.F. Tedder, H. Karasuyama, A. Miyawaki, T. Adachi, Intravital imaging of Ca(2+) signals in lymphocytes of Ca(2+) biosensor transgenic mice: indication of autoimmune diseases before the pathological onset, Sci. Rep. 6 (2016) 18738.
[18] M. Okazawa, K. Takao, A. Hori, T. Shiraki, K. Matsumura, S. Kobayashi, Ionic basis of cold receptors acting as thermostats, J. Neurosci. 22 (2002) 3994–4001.
[19] K. Venkatachalam, C. Montell, TRP channels, Annu. Rev. Biochem. 76 (2007) 387–417.
[20] P.R. de Jong, N. Takahashi, A.R. Harris, J. Lee, S. Bertin, J. Jeffries, M. Jung, J. Duong, A.I. Triano, Y. Niv, D.S. Herdman, K. Taniguchi, C.W. Kim, H. Dong, L. Eckmann, S.M. Stanford, N. Bottini, M. Corr, E. Raz, Ion channel TRPV1-dependent activation of PTP1B suppresses EGFR-associated intestinal tumorigenesis, J. Clin. Investig. 124 (2014) 3793–3806.
[21] A. Leffler, M.J. Fischer, D. Rehner, S. Kienel, K. Kistner, S.K. Sauer, N.R. Gavva, P.W. Reeh, C. Nau, The vanilloid receptor TRPV1 is activated and sensitized by local anesthetics in rodent sensory neurons, J. Clin. Investig. 118 (2008) 763–776.
[22] J. Chen, L. Li, Y. Li, X. Liang, Q. Sun, H. Yu, J. Zhong, Y. Ni, Z. Zhao, P. Gao, B. Wang, D. Liu, Z. Zhu, Z. Yan, Activation of TRPV1 channel by dietary capsaicin improves visceral fat remodeling through connexin43-mediated Ca2+ influx, Cardiovasc. Diabetol. 14 (2015) 22.
[23] J. Kupari, M. Haring, E. Agirre, G. Castelo-Branco, P. Ernfors, An atlas of vagal sensory neurons and their molecular specialization, Cell Rep. 27 (2019) 2508–2523, e2504.
[24] G. Buzsaki, C.A. Anastassiou, C. Koch, The origin of extracellular fields and currents–EEG, ECoG, LFP and spikes, Nat. Rev. Neurosci. 13 (2012) 407–420.
[25] M. Costa, G.W. Hennig, S.J. Brookes, Intestinal peristalsis: a mammalian motor pattern controlled by enteric neural circuits, Ann. N. Y. Acad. Sci. 860 (1998) 464–466.
[26] J.F. Cryan, T.G. Dinan, Mind-altering microorganisms: the impact of the gut microbiota on brain and behaviour, Nat. Rev. Neurosci. 13 (2012) 701–712.
[27] P. Holzer, TRP channels in the digestive system, Curr. Pharmaceut. Biotechnol. 12 (2011) 24–34.
[28] S.K. Panchal, E. Bliss, L. Brown, Capsaicin in metabolic syndrome, Nutrients 10 (2018).
[29] P. Geppetti, M. Trevisani, Activation and sensitisation of the vanilloid receptor: role in gastrointestinal inflammation and function, Br. J. Pharmacol. 141 (2004) 1313–1320.